Graphene-based thermal interface materials with high through-plane thermal conductivity inspired by Baumkuchen

Applied Physics Letters

RESEARCH ARTICLE | MARCH 09 2026

Graphene-based thermal interface materials with high through-plane thermal conductivity inspired by Baumkuchen

Special Collection: Thermal Properties of Graphene and Carbon Materials – From Physics to Applications in Thermal Management

Sihua Guo ; Minghe Wang ; Si Chen; Kristoffer Harr ; Yong Zhang ; Yan Zhang ; Bin Wei ; Johan Liu

Appl. Phys. Lett. 128, 102201 (2026)
https://doi.org/10.1063/5.0310419

AIP Publishing

Applied Physics Letters ARTICLE pubs.aip.org/aip/apl

Graphene-based thermal interface materials with high through-plane thermal conductivity inspired by Baumkuchen

Cite as: Appl. Phys. Lett. **128**, 102201 (2026); doi: 10.1063/5.0310419
Submitted: 2 November 2025 · Accepted: 22 January 2026 ·
Published Online: 9 March 2026

Sihua Guo,[1] Minghe Wang,[1] Si Chen,[2] Kristoffer Harr,[3] Yong Zhang,[1,a)] Yan Zhang,[1,a)] Bin Wei,[1,a)] and Johan Liu[4,a)]

AFFILIATIONS

[1]SMIT Center, School of Mechatronics Engineering and Automation, Shanghai University, 20 Chengzhong Rd., Shanghai 201800, People's Republic of China
[2]Shanghai Ruixi New Materials High Tech Co. Ltd., No 818, Chuhua North Road, Shanghai, People's Republic of China
[3]SHT Smart High-Tech AB, Terminalvägen 12, SE-418 79 Gothenburg, Sweden
[4]Electronics Materials and Systems Laboratory, Department of Microtechnology and Nanoscience, Chalmers University of Technology, Kemivägen 9, SE 412 96 Gothenburg, Sweden

Note: This paper is part of the Special Topic, Thermal Properties of Graphene and Carbon Materials â From Physics to Applications in Thermal Management.
[a)]**Authors to whom correspondence should be addressed:** yongz@shu.edu.cn; yzhang@shu.edu.cn; bwei@shu.edu.cn; and jliu@chalmers.se

ABSTRACT

To enhance the thermal management capabilities of epoxy composite, inspired by Baumkuchen, a simple, scalable, and environmentally friendly process was proposed. The graphene strips, without any chemical modification, were integrated into assembled graphene paper, and the vertically aligned graphene strips/epoxy composite with the tree-ring structure was prepared by the rolling cutting method. The composite exhibited an extremely high through-plane thermal conductivity of 49.2 W/mK, which was 289 times higher than that of pure EP. Additionally, the composite also possesses a range of desirable properties, including good electromagnetic interference shielding, efficient Joule heating, and remarkable mechanical performance. These properties further expand the application of graphene-based thermal interface materials in the field of thermal management of electronic devices.

The rapid development of 5G technology has exacerbated the thermal management challenges of electronic devices, leading to an increasing demand for high-performance thermal interface materials (TIMs).[1–4] Polymers are widely used in thermal management applications due to their advantages such as low weight, low cost, corrosion resistance, and ease of processing. They are usually composed of high thermal conductivity fillers such as metals,[5,6] ceramics,[7,8] and carbon materials.[9,10] Graphene, with its extremely high in-plane thermal conductivity, has become one of the most promising candidate materials.[11–15] Liang *et al.*[16] noted that, among the various graphene-based composites employed for thermal management, the most common approach is to incorporate graphene as a filler into polymers. It has been reported that directly dispersing graphene in the polymer can achieve a thermal conductivity of 0.39 W/mK in the composite.[17] Additionally, functionalized graphene can further enhance the thermal conductivity of the composite. For instance, Lin *et al.*[18] prepared p-phenylenediamine modified graphene/epoxy composites with a thermal conductivity of 1.7 W/mK. However, the functionalization of graphene has a limited effect on enhancing the thermal conductivity of composites because functionalization also reduces the intrinsic thermal conductivity of graphene due to the increased phonon scattering caused by functional groups.[19] Phonon transport is the primary mode of heat transfer. Therefore, the key to improving thermal conductivity lies in reducing the phonon scattering rate and the interfacial thermal resistance. Liang *et al.*[16] indicated that constructing phonon transport pathways remains a topic for future research. Currently, there are

many methods for constructing through-plane three-dimensional heat conduction networks, such as directional freezing,[20,21] magnetic fields,[22] chemical vapor deposition,[23,24] electrospinning,[25,26] electrostatic flocking,[27] 3D printing,[28] force fields,[29,30] etc. For example, aligning graphene nanoplatelets in polyvinyl alcohol using a rotating magnetic field significantly enhanced the through-plane thermal conductivity of the composite.[22] Additionally, in an electric field-assisted plasma-enhanced chemical vapor deposition system, chloroform was used to assist the rapid growth of vertically aligned graphene arrays. This excellent framework endowed TIM with excellent vertical thermal conductivity.[31] However, these technologies generally face limitations such as complex operation, use of toxic solvents, and high cost, which hinder their industrialization and cannot meet the requirements of modern thermal management applications.

The thermal conductivity of graphene generally increases with increasing sample size because of the low intrinsic phonon scattering.[19] Moreover, larger-sized graphene fillers help to reduce the number of interfaces and thermal resistance.[32,33] Therefore, compared to nano- and micro-sized graphene, macroscopic graphene films can effectively construct thermal transport pathways, significantly enhancing the thermal conductivity of the composite. Vertically aligned graphene film/polydimethylsiloxane composites exhibited exceptionally high thermal conductivity.[34] Furthermore, the perpendicular thermal conductivity of the composite made of hybrid bilayer strips consisting of porous polymer foam adhered to graphene paper is 276 W/mK.[35] However, the high cost of whole graphene films weakens their cost competitiveness in practical thermal management applications. Large amounts of graphene waste are generated during the commercial-scale production of graphene-enhanced TIM. Recycling and reusing graphene waste not only retains its original properties but also reduces costs and minimizes environmental pollution caused by the accumulation of such industrial waste. Meanwhile, Shen *et al.*[36] proposed that when the size of graphene exceeds a certain critical value (e.g., a few micrometers), the intrinsic thermal conductivity of pristine graphene becomes more significant, and the functionalization of graphene is ineffective in enhancing the thermal conductivity of the composite.

Inspired by the structure of Baumkuchen, this study utilized graphene strips (GS) without any chemical modification to fabricate the vertically aligned GS/epoxy (VGS/EP) composite with a tree-ring structure, which exhibited excellent through-plane thermal conductivity. Oriented graphene, as a direct heat conduction pathway, enables heat to be transferred effectively along the pathway, thereby improving the thermal conductivity of the composite. At the same time, the composite exhibited a range of interesting multifunctional properties, including good electromagnetic interference (EMI) shielding, efficient Joule heating, and impressive mechanical properties.

Figure 1 illustrates the process of preparing VGS/EP composite inspired by Baumkuchen in Fig. S3 (for more details, refer to the supplementary material). Three different experiments were conducted to compare the enhancement effects of graphene size and arrangement on the thermal conductivity of graphene-based composite. First, the thermal resistance of three composites with the same graphene content at 80 °C and different pressures was studied in Fig. 2(a). As the pressure increased, the thermal resistance gradually decreased and leveled off. Since the assembly pressure of electronic devices is generally 40 psi, the thermal resistance at 40 psi was selected to obtain the thermal conductivity of the composite. Figure 2(b) compares the thermal conductivity

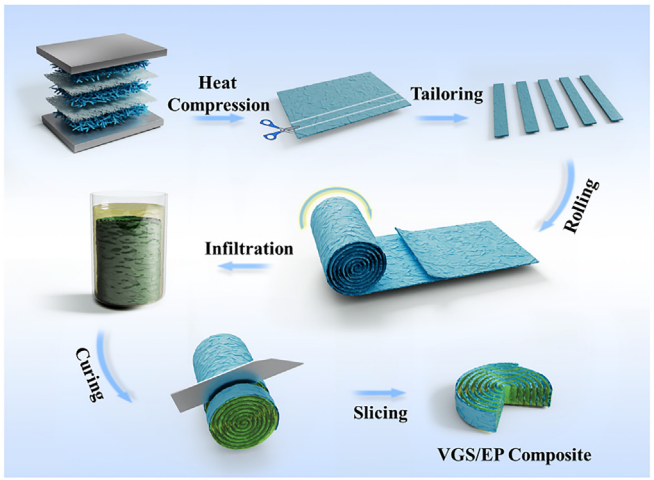

FIG. 1. A schematic illustration of the manufacturing procedure for the VGS/EP composite.

of pure EP and three graphene-based composites with a filler content of 10 wt. %. The EP exhibited a thermal conductivity of 0.17 W/mK. The thermal conductivity of GP/EP, RGS/EP, and VGS/EP composite was 0.56 W/mK, 2.11 W/mK, and 6.65 W/mK, which were 3.3, 12.4, and 39.1 times that of pure EP, respectively. To visually observe the internal structures of graphene-based composite, Figs. 2(c)–2(e) display the cross-sectional scanning electron microscope (SEM) images of GP/EP, RGS/EP, and VGS/EP composites. Due to the small size of graphene powder, graphene is randomly distributed within the polymer, creating numerous interfaces and forming a discontinuous thermal conductive network in the GP/EP composite in Fig. 2(c). However, the increase in the graphene filler size is beneficial to the formation of partial thermal conductive channels in the RGS/EP composite, as shown in Fig. 2(d). Importantly, the VGS/EP composite exhibits a vertically arranged graphene structure in Fig. 2(e). This suggests that incorporating oriented graphene frameworks into the EP matrix can significantly enhance the thermal conductivity of the composite.

The heat flux distribution of three kinds of graphene-based composite in Fig. 2(f) as well as the temperature distribution of VGS/EP composite with tree-ring structure in Fig. 2(g) was simulated by the finite element simulation (for more modeling details, refer to the supplementary material). The vertically oriented graphene provides a fast channel for heat conduction, further confirming that the construction of directional heat conduction channels promotes a significant improvement in the thermal conductivity of the composite.

Additionally, a low coefficient of thermal expansion (CTE) helps to reduce thermal stress generated during the long-term thermal cycling, generally requiring no more than 150 ppm/K.[37] As shown in Fig. 2(h), the CTE of pure EP was as high as 65 ppm/K. The corresponding CTE of GP/EP, RGS/EP, and VGS/EP composites was reduced to 55, 44, and 39 ppm/K, respectively. Insufficient mechanical properties of TIM lead to many adverse consequences, such as failure under mechanical stress and difficulties in processing and application.[38,39] Especially, the vertically oriented graphene structure in VGS/EP composite significantly reduces the CTE, reflecting the importance of directional heat conduction structure.

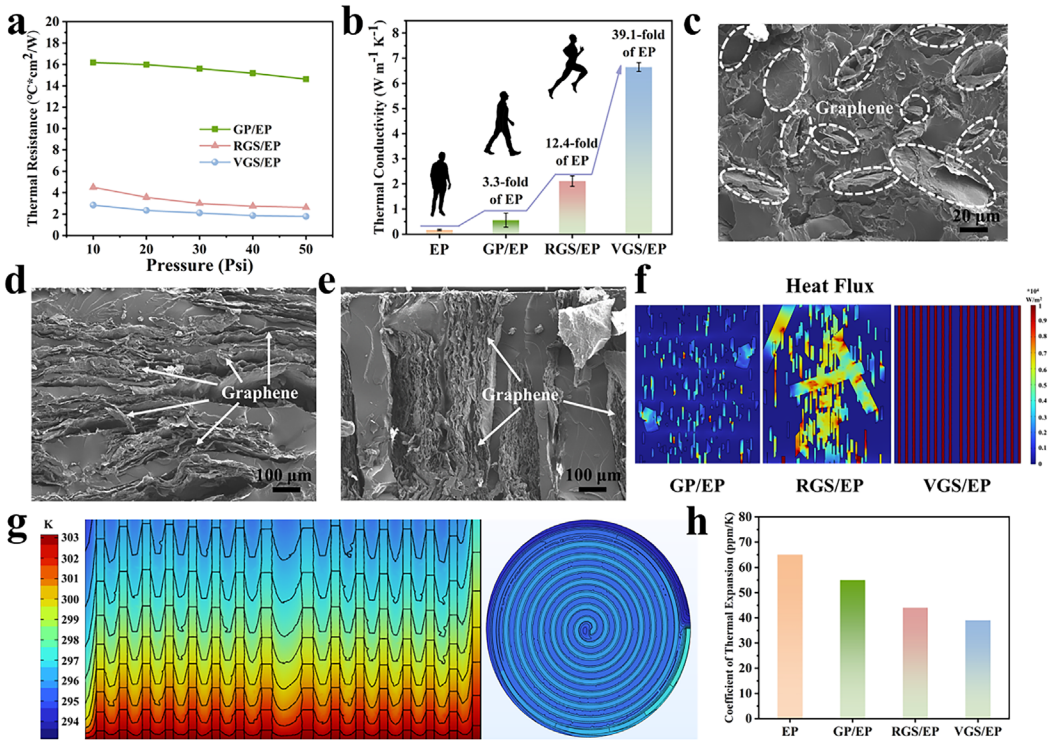

FIG. 2. (a) Thermal resistance of the various composites at different pressures. (b) Comparison of thermal conductivity between pure EP and graphene-based composite. Cross-sectional SEM morphology of (c) GP/EP, (d) RGS/EP, and (e) VGP/EP composites. (f) Heat flux distribution of the composite simulated by finite element simulation. (g) Temperature distributions in the VGS/EP composite were simulated by finite element simulation. (h) The coefficient of thermal expansion of pure EP and graphene-based composite.

The thermal conductivity of VGS/EP composite increases with the increase in filler content. Notably, at a graphene content of 40 wt. %, the through-plane thermal conductivity of the VGS/EP composite reached an impressive 49.2 W/mK, which was 289 times higher than that of pure EP, as shown in Fig. 3(a). To explain the reason for this amazing thermal conductivity, Figs. 3(c)–3(e) show the cross-sectional SEM images of the VGS/EP composite with the tree-ring structure in Fig. 3(b). The vertically arranged graphene provided numerous thermal conductive pathways that can rapidly transfer heat from the hot end to the cold end, thereby enhancing the heat transfer efficiency. Figure 3(f) summarizes the through-plane thermal conductivity of previously reported composites to demonstrate the advantages of this structure for the VGS/EP composite (more details in Table S1, see the supplementary material). The thermal conductivity of the VGS/EP composite significantly surpasses that of most previously reported composites, demonstrating its superior capability in enhancing the thermal conductivity of the composite. In addition, the thermal resistance (1 mm thickness, 40 psi pressure) in Fig. 3(g), surface roughness in Fig. 3(h), and CTE in Fig. 3(i) of the VGS/EP composite with different filler contents were studied. It found that the VGS/EP composite exhibited a thermal resistance of 0.29 Kcm^2/W, a surface roughness of 1.08 μm, and a CTE of 17 ppm/K at a graphene content of 40 wt. %. Interestingly, this composite with high through-plane thermal conductivity, low thermal resistance, low surface roughness, and low CTE demonstrates fascinating advantages in commercial applications.

The cooling efficiency of the VGS/EP composite and commercial thermally conductive silicone pads was tested under actual working conditions using a 20 W light emitting diode (LED) chip. To evaluate the heat dissipation performance, the TIM was placed between the LED chip and the aluminum heat sink in Fig. S7.[40] The temperature variation on the top surface of the LED chip over time was recorded by an infrared thermal imager in Fig. 4(a). The operating temperature of the LED chip without TIM increased sharply and finally stabilized at 64 °C. In contrast, the temperature of the LED chip combined with the commercial thermal conductive silicone pad rose slowly and reached equilibrium after 50 s, and the operating temperature was significantly reduced to 56 °C. The temperature of the LED chip integrated with the VGS/EP composite stabilized at 48 °C, which was 16 and 8 °C lower than the temperature of the LED chip without TIM and with a commercial thermal silicone pad, respectively, in Fig. 4(b). Overall, the carefully designed TIM with tree-ring structure provided an effective solution for high-performance thermal management applications in advanced packaging technologies.

In addition to excellent thermal properties, the VGS/EP composite also exhibited good electrothermal conversion performance. Figure 4(c) shows the relationship between the surface temperature of VGS/EP composite and time under an applied voltage ranging from 1 to 5 V. As the applied voltage increases, the surface temperature of the

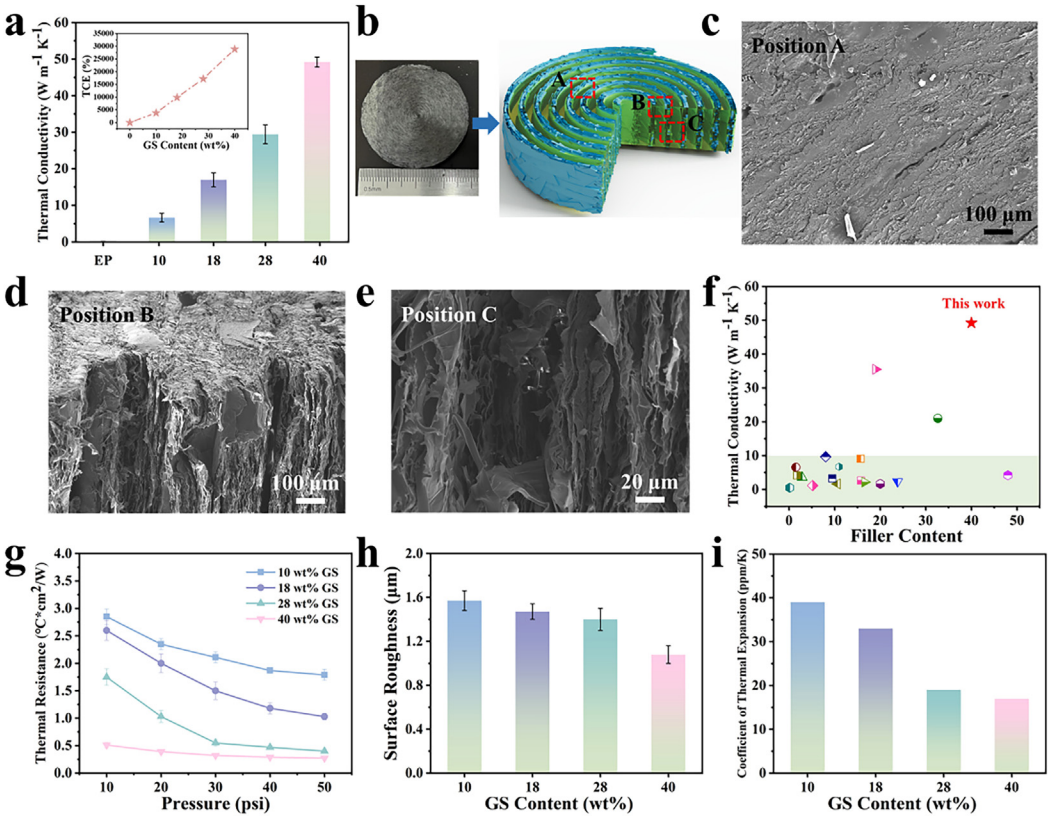

FIG. 3. (a) The thermal conductivity of the composite and thermal conductive enhancements (TCEs) of the VGS/EP composite. (b) Photograph and diagrammatic representation of the VGS/EP composite. (c)–(e) Corresponding SEM micrographs that exhibit the microstructure of the VGS/EP composite. (f) Comparison of the thermal conductivities for the VGS/PE composite and other composites reported in previous studies. (g) Thermal resistance of the VGS/EP composite with various GS contents at different pressures. (h) Surface roughness of the VGS/EP composite with different GS contents. (i) The CTE of the VGS/EP composite with various GS contents.

VGS/EP composite also increases accordingly. When the applied voltage was 5 V, the stable surface temperature of the composite reached 55 °C. The stable temperature of the composite was positively correlated with the applied voltage in Fig. 4(d), which was in accordance with Joule's law:[41]

$$Q = \frac{U^2 T}{R}, \tag{1}$$

where Q is the heat generated, U is the applied voltage, R is the resistance, and T is the working time.

The insufficient mechanical properties of TIM can lead to many adverse effects, such as failure under mechanical stress and difficulties in processin and application. Therefore, good mechanical properties are crucial for TIM.[42] Figure 5(a) shows that the compressive strength of VGS/EP composite decreased with the increase in graphene content. At a graphene content of 40 wt. %, the compressive strength of VGS/EP composite under a compressive strain of 50% was 6.13 MPa. A high content of EP can effectively fill micro-defects and voids, thereby enhancing the overall strength of the composite.

Since interlaminar shear is the weakest link in the "annular-cylindrical" structure, the three-point bending method can simultaneously induce tension, compression, and interlaminar shear in a single specimen, making it the most effective method for triggering rolling slip and delamination energy dissipation. Therefore, in addition to compression testing, we also adopted this method and quantified toughness as the area under the flexural stress-strain curve. As shown in Figs. 5(b) and 5(c), the flexural strength and toughness of pure EP reached 150.66 MPa and 3.83 MJ/m^3, respectively, both superior to VGS/EP composite. The flexural toughness of the VGS/EP composite first increases and then decreases with the increase in the GS content. Pure EP achieves high toughness through molecular chain plasticity. However, the introduction of graphene rolls increases interfacial defects and restricts matrix deformation due to the high-modulus framework, resulting in a decrease in overall toughness. At low content, the roll spacing is moderate, the slip-deflection mechanism is activated, the curve shows a plateau, and the toughness slightly recovers. Conversely, adjacent axial surfaces contact and form a rigid framework. Interfacial debonding occurs, the surface is "bridged and locked" by adjacent surface before sliding, causing a sharp reduction in frictional stroke, the plateau disappears, and toughness decreases again.

With the continuous advancement of electronic equipment and communication technology, the research and application of electromagnetic shielding materials are becoming increasingly important.[43,44] Figure 5(d) shows the EMI shielding performance of the VGS/EP

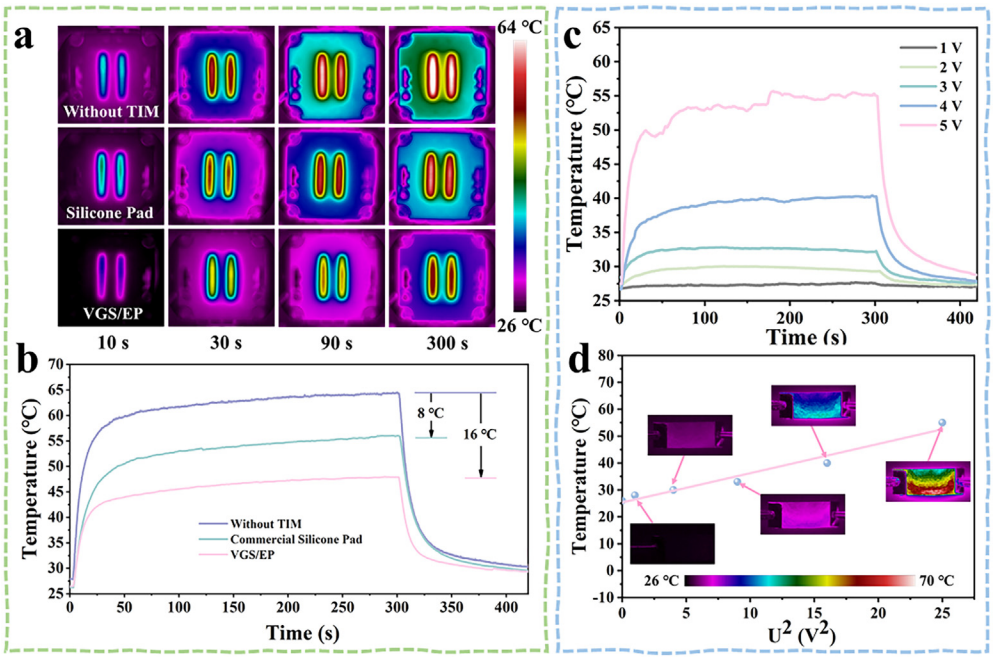

FIG. 4. (a) An infrared thermal image of LED modules captured with a thermal imaging camera. (b) Temperature curves of LED modules during the heating phase and the subsequent natural cooling phase, without TIM, with a commercial silicone pad, and with VGS/EP composite, respectively. (c) The surface temperature of the VGS/EP composite is plotted against time for various input voltages. (d) Experimental temperature data along with linear analysis for the relationship between temperature and U^2.

composite with 40 wt. % GS content in the X-band (8.2–12.4 GHz), and it is placed in a Tesla coil system to verify the actual shielding capability of the VGS/EP composite against electromagnetic waves (EMWs) in Fig. S8. Figure 5(e) illustrates the EMI shielding mechanism of the VGS/EP composite. When EMWs propagate through different media, they encounter varying electromagnetic impedance.[45] If the impedance of two media does not match, part of the waves is reflected, while the remaining EMWs pass through the

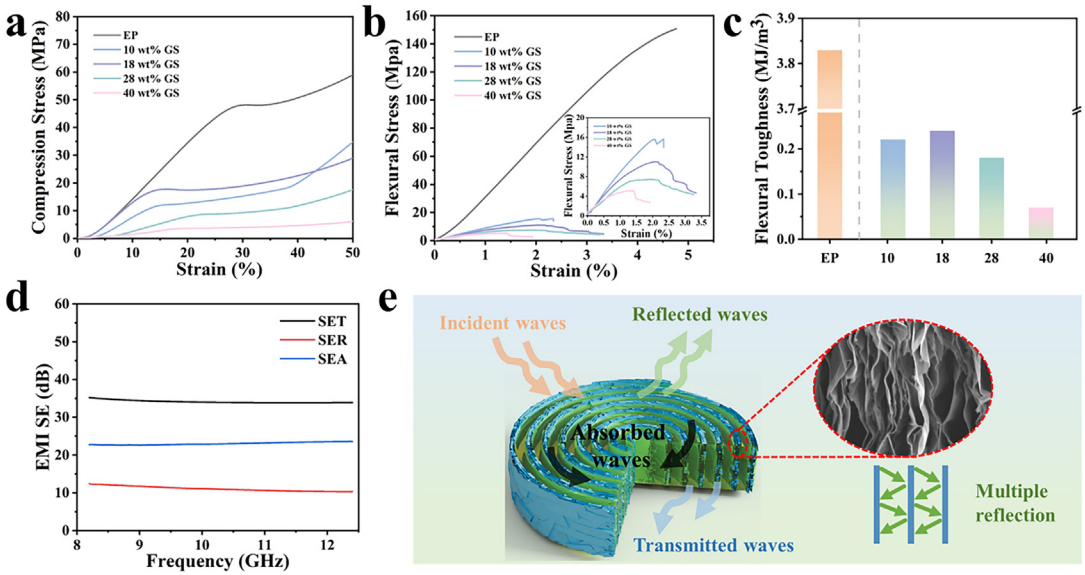

FIG. 5. (a) Compression stress-strain curves for the VGS/EP composite with different GS contents. (b) Flexural stress-strain curves of pure EP and VGS/EP composites with different GS contents. (c) The flexural toughness of the pure EP and VGS/EP composites with different GS contents. (d) The electromagnetic interference (EMI) shielding effectiveness of the VGS/EP composite at the 40 wt. % GS content. (e) A depiction of the EMI shielding mechanism for the VGS/EP composite.

interconnected graphene framework. The parallel alignment of graphene promotes interfacial polarization, in which the movement and oscillation of charge carriers generate energy losses. This effectively attenuates the EMWs into heat and reduces their propagation, thereby enhancing the shielding efficiency.[43,46,47]

In summary, this study developed a VGS/EP composite with a tree-ring structure. The highly vertical alignment and dense layered structure provide an efficient pathway for heat transfer. The composite exhibited an impressive through-plane thermal conductivity of 49.2 W/mK and a low thermal resistance of 0.29 Kcm^2/W (1 mm thickness, 40 psi pressure). Practical tests have shown that the VGS/EP composite exhibits excellent heat dissipation performance, significantly reducing the temperature of the LED chip by 16 °C compared to using a bare LED chip. Furthermore, the composite displayed good EMI shielding, efficient Joule heating, excellent mechanical properties, and a low CTE. The significance of this study lies in reusing graphene waste to prepare graphene-based TIM, providing a solution for thermal management applications in electronic devices.

See the supplementary material for the details on the experimental section, the process of finite element simulation, the comparison of the thermal conductivity of various composite materials in the literature, the practical applications of heat transfer, and the practical applications of electromagnetic shielding.

We acknowledge the financial support from the Production Area of Advance at Chalmers University of Technology, Sweden, and the financial support from the Shanghai Science and Technology Commission (Contract No. 22501100300).

AUTHOR DECLARATIONS

Conflict of Interest

The authors have no conflicts to disclose.

Author Contributions

Sihua Guo and Minghe Wang contributed equally to this paper.

Sihua Guo: Conceptualization (lead); Data curation (lead); Formal analysis (lead); Investigation (lead); Writing – original draft (lead). **Minghe Wang:** Conceptualization (equal); Data curation (equal). **Si Chen:** Investigation (supporting). **Kristoffer Harr:** Investigation (supporting). **Yong Zhang:** Supervision (equal); Writing – review & editing (equal). **Yan Zhang:** Supervision (equal); Writing – review & editing (equal). **Bin Wei:** Supervision (lead). **Johan Liu:** Funding acquisition (lead); Resources (lead); Supervision (lead); Writing – review & editing (lead).

DATA AVAILABILITY

The data that support the findings of this study are available from the corresponding authors upon reasonable request.

REFERENCES

[1]Q. Cui, X. Ma, Z. You, X. Yang, Y. Zhang, and J. Wei, "Bending the heat: Innovative ultra-thin flexible loop heat pipes for enhanced mobile device cooling," Energy Convers. Manage. **325**, 119332 (2025).
[2]Y. Jing, H.-Q. Liu, F. Zhou, F.-N. Dai, and Z.-S. Wu, "Design, progress and challenges of 3D carbon-based thermally conductive networks," New Carbon Mater. **39**(5), 844–871 (2024).
[3]T. Yang, J. Leng, J. Hu, P. Wang, M. Edeleva, L. Cardon, Z. Yan, T. Wang, and J. Zhang, "Enhancing thermal conductivity and balancing mechanical properties of 3D-printed iPP/HDPE-based dielectric composites via the introduction of hybrid fillers and tailored crystalline structure," Virtual Phys. Prototyping **18**(1), e2230215 (2023).
[4]W. Chen, J. Wu, Y. Cao, Y. Liu, and F. Xu, "Highly thermal conductivity polymer composites reinforced by BNNS/UHMWPE fabric for reliable electronic thermal protection and management," Compos. Commun. **49**, 101991 (2024).
[5]W. Yang, Y. Du, Q. Deng, S. Li, C. Li, J. Tian, P. Chen, T. Fu, Y. Luo, Y. Zhang, S. Zhu, X. Liu, Z. Rao, and X. Li, "High thermal conductivity composite phase change material with Zn^{2+} metal organic gel and expanded graphite for battery thermal management," Appl. Therm. Eng. **249**, 123358 (2024).
[6]H.-A. Cha, S.-J. Ha, M.-G. Jo, Y. K. Moon, J.-J. Choi, B.-D. Hahn, C.-W. Ahn, and D. K. Kim, "Three-dimensional MgO filler networking composites with significantly enhanced thermal conductivity," Adv. Compos. Hybrid Mater. **7**(5), 178 (2024).
[7]L. Alexis, J. Lee, G. A. Alvarez, S. Awale, D. S. Jesus, M. Lizcano, and Z. Tian, "Significantly enhanced thermal conductivity of hBN/PTFE composites: A comprehensive study of filler size and dispersion," ACS Appl. Mater. Interfaces **16**(22), 29042–29048 (2024).
[8]B. Wu, R. Chen, R. Fu, S. Agathopoulos, X. Su, and H. Liu, "Low thermal expansion coefficient and high thermal conductivity epoxy/Al_2O_3/T-ZnOw composites with dual-scale interpenetrating network structure," Composites, Part A **137**, 105993 (2020).
[9]C. Feng, H. Liu, Z. Hang, Y. Su, X. Xia, and G. J. Weng, "Study on thermal conductivity of 0D/1D/2D carbon filler reinforced cement composites with phonon physical model," Cem. Concr. Compos. **157**, 105917 (2025).
[10]Z. Zhang, R. Yang, Y. Wang, K. Xu, W. Dai, J. Zhang, M. Li, L. Li, Y. Guo, Y. Qin, B. Zhu, Y. Zhou, X. Wang, T. Cai, C.-T. Lin, K. Nishimura, H. N. Li, N. Jiang, and J. Yu, "Enhanced thermal conductivity and reduced thermal resistance in carbon fiber-based thermal interface materials with vertically aligned structure," J. Mater. Chem. A **12**(36), 24428–24440 (2024).
[11]S. Guo, S. Chen, A. Nkansah, A. Zehri, M. Murugesan, Y. Zhang, Y. Zhang, C. Yu, Y. Fu, M. Enmark, J. Chen, X. Wu, W. Yu, and J. Liu, "Toward ultrahigh thermal conductivity graphene films," 2D Mater. **10**(1), 014002 (2023).
[12]D. L. Nika, E. P. Pokatilov, A. S. Askerov, and A. A. Balandin, "Phonon thermal conduction in graphene: Role of Umklapp and edge roughness scattering," Phys. Rev. B **79**, 155413 (2009).
[13]A. A. Balandin, "Thermal properties of graphene and nanostructured carbon materials," Nat. Mater. **10**, 569–581 (2011).
[14]K. M. F. Shahil and A. A. Balandin, "Graphene−multilayer graphene nanocomposites as highly efficient thermal interface materials," Nano Lett. **12**(2), 861–867 (2012).
[15]D. L. Nika and A. A. Balandin, "Phonons and thermal transport in graphene and graphene-based materials," Rep. Prog. Phys. **80**, 036502 (2017).
[16]C. Liang, J. Hong, C. Wan, X. Ma, Z. Wang, X. Zhao, A. Hou, D. Nika, Y. Huo, and G. Zhang, "A perspective on mechanism of heat transfer and performance optimization in advanced thermal interface materials," Appl. Phys. Lett. **126**, 070501 (2025).
[17]L. X. Zhi, M. S. A. Majid, M. J. M. Ridzuan, M. S. Ismail, M. D. Azaman, and A. Khasri, "Effect of dispersion methods on electromagnetic interference shielding effectiveness and thermal conductivity of graphene bio-based epoxy composites," Polym. Compos. **45**(15), 13721–13736 (2024).
[18]J. Lin, J. Zhou, M. Guo, D. Chen, and G. Chen, "Study on thermal conductivity of P-phenylenediamine modified graphene/epoxy composites," Polymers **14**(17), 3660 (2022).
[19]X. Huang, C. Zhi, Y. Lin, H. Bao, G. Wu, P. Jiang, and Y.-W. Mai, "Thermal conductivity of graphene-based polymer nanocomposites," Mater. Sci. Eng., R **142**, 100577 (2020).
[20]B. Hu, W. Zhang, H. Guo, S. Xu, Y. Li, M. Li, and B. Li, "Nacre-mimetic elastomer composites with synergistic alignments of boron nitride/graphene oxide towards high through-plane thermal conductivity," Composites, Part A **156**, 106891 (2022).

[21]G. Lian, C.-C. Tuan, L. Li, S. Jiao, Q. Wang, K.-S. Moon, D. Cui, and C.-P. Wong, "Vertically aligned and interconnected graphene networks for high thermal conductivity of epoxy composites with ultralow loading," Chem. Mater. **28**(17), 6096–6104 (2016).
[22]S. Cheng, X. Guo, P. Tan, M. Lin, J. Cai, Y. Zhou, D. Zhao, W. Cai, Y. Zhang, and X.-A. Zhang, "Aligning graphene nanoplates coplanar in polyvinyl alcohol by using a rotating magnetic field to fabricate thermal interface materials with high through-plane thermal conductivity," Composites, Part B **264**, 110916 (2023).
[23]S. Xu, S. Wang, Z. Chen, Y. Sun, Z. Gao, H. Zhang, and J. Zhang, "Electric-field-assisted growth of vertical graphene arrays and the application in thermal interface materials," Adv. Funct. Mater. **30**(34), 2003302 (2020).
[24]Q. Yan, F. E. Alam, J. Gao, W. Dai, X. Tan, L. Lv, J. Wang, H. Zhang, D. Chen, K. Nishimura, L. Wang, J. Yu, J. Lu, R. Sun, R. Xiang, S. Maruyama, H. Zhang, S. Wu, N. Jiang, and C. T. Lin, "Soft and self-adhesive thermal interface materials based on vertically aligned, covalently bonded graphene nanowalls for efficient microelectronic cooling," Adv. Funct. Mater. **31**(36), 2104062 (2021).
[25]J. Huo, G. Zhang, X. Yuan, and S. Guo, "Electrospraying graphene nanosheets on polyvinyl alcohol nanofibers for efficient thermal management materials," ACS Appl. Nano Mater. **6**(7), 6241–6246 (2023).
[26]J. Liang, J. Luo, J. Zhang, Y. Xiong, and S. Tan, "Constructing a high-density thermally conductive network through electrospinning–hot-pressing of BN@PDA/GO/PVDF composites," ACS Appl. Polym. Mater. **4**(4), 2414–2422 (2022).
[27]K. Uetani, S. Ata, S. Tomonoh, T. Yamada, M. Yumura, and K. Hata, "Elastomeric thermal interface materials with high through-plane thermal conductivity from carbon fiber fillers vertically aligned by electrostatic flocking," Adv. Mater. **26**(33), 5857–5862 (2014).
[28]J. Jing, Y. Chen, S. Shi, L. Yang, and P. Lambin, "Facile and scalable fabrication of highly thermal conductive polyethylene/graphene nanocomposites by combining solid-state shear milling and FDM 3D-printing aligning methods," Chem. Eng. J. **402**, 126218 (2020).
[29]X. Zhang, X. Xie, X. Cai, Z. Jiang, T. Gao, Y. Ren, J. Hu, and X. Zhang, "Graphene−perfluoroalkoxy nanocomposite with high through-plane thermal conductivity fabricated by hot-pressing," Nanomaterials **9**(9), 1320 (2019).
[30]X. Guo, S. Cheng, K. Xu, B. Yan, Y. Li, W. Cai, J. Cai, B. Xu, Y. Zhou, Y. Zhang, and X. A. Zhang, "Controlling anisotropic thermal properties of graphene aerogel by compressive strain," J. Colloid Interface Sci. **619**, 369–376 (2022).
[31]S. Xu, T. Cheng, Q. Yan, C. Shen, Y. Yu, C. T. Lin, F. Ding, and J. Zhang, "Chloroform-assisted rapid growth of vertical graphene array and its application in thermal interface materials," Adv. Sci. **9**(15), 2200737 (2022).
[32]F. Chen, P. Yu, l Mao, and J. Wang, "Simple large-scale method of recycled graphene films vertical arrangement for superhigh through-plane thermal conductivity of epoxy composites," Compos. Sci. Technol. **215**, 109026 (2021).
[33]B. Tang, G. Hu, H. Gao, and L. Hai, "Application of graphene as filler to improve thermal transport property of epoxy resin for thermal interface materials," Int. J. Heat Mass Transfer **85**, 420–429 (2015).
[34]Y.-F. Zhang, D. Han, Y.-H. Zhao, and S.-L. Bai, "High-performance thermal interface materials consisting of vertically aligned graphene film and polymer," Carbon **109**, 552–557 (2016).
[35]X. Tan, J. Ying, J. Gao, Q. Yan, L. Lv, K. Nishimura, Q. Wei, H. Li, S. Du, B. Wu, R. Xiang, J. Yu, N. Jiang, C.-T. Lin, and W. Dai, "Rational design of high-performance thermal interface materials based on gold-nanocap-modified vertically aligned graphene architecture," Compos. Commun. **24**, 100621 (2021).
[36]X. Shen, Z. Wang, Y. Wu, X. Liu, and J.-K. Kim, "Effect of functionalization on thermal conductivities of graphene/epoxy composites," Carbon **108**, 412–422 (2016).
[37]N. Wu, S. Che, P. Shen, N. Chen, F. Chen, G. Ma, H. Liu, W. Yang, X. Wang, and Y. Li, "A binder-free ice template method for vertically aligned 3D boron nitride polymer composites towards thermal management," J. Colloid Interface Sci. **647**, 43–51 (2023).
[38]Z. Shi, X. F. Li, H. Bai, W. W. Xu, S. Y. Yang, Y. Lu, J. J. Han, C. P. Wang, X. J. Liu, and W. B. Li, "Influence of microstructural features on thermal expansion coefficient in graphene/epoxy composites," Heliyon **2**(3), e00094 (2016).
[39]S. Wang, M. Tambraparni, J. Qiu, J. Tipton, and D. Dean, "Thermal expansion of graphene composites," Macromolecules **42**(14), 5251–5255 (2009).
[40]Z. G. Wang, Y. Huo, H. F. Nan, G. Zhang, J. Gao, L. Xu, C. H. Li, J. Z. Xu, and Z. M. Li, "Constructing the snail shell-like framework in thermal interface materials for enhanced through-plane thermal conductivity," ACS Appl. Mater. Interfaces **16**(36), 48386–48394 (2024).
[41]X. Hao, D. Li, X. Peng, W. Lan, and C. Liu, "In situ construction of biomass derived 3D carbon framework for efficient electromagnetic interference shielding and Joule heating performance," Chem. Eng. J. **479**, 147681 (2024).
[42]D. Liu, Q.-Q. Kong, H. Jia, L.-J. Xie, J. Chen, Z. Tao, Z. Wang, D. Jiang, and C.-M. Chen, "Dual-functional 3D multi-wall carbon nanotubes/graphene/silicone rubber elastomer: Thermal management and electromagnetic interference shielding," Carbon **183**, 216–224 (2021).
[43]Z. Cui, M. Yang, G. Han, H. Zhang, Y. Wang, Y. Zhang, Z. Li, J. He, R. Yu, J. Shui, and X. Liu, "Recent advances in carbon composite films for high-performance, multifunctional and intelligent electromagnetic interference shielding and electromagnetic wave absorption," Carbon **230**, 119627 (2024).
[44]J. Zhang, J. Zhang, X. Shuai, R. Zhao, T. Guo, K. Li, D. Wang, C. Ma, J. Li, and J. Du, "Design and synthesis strategies: 2D materials for electromagnetic shielding/absorbing," Chem. - Asian J. **16**(23), 3817–3832 (2021).
[45]Y. Zhang, K. Ruan, and J. Gu, "Flexible sandwich-structured electromagnetic interference shielding nanocomposite films with excellent thermal conductivities," Small **17**(42), 2101951 (2021).
[46]Y. Li, D. Zhang, B. Zhou, C. He, B. Wang, Y. Feng, and C. Liu, "Synergistically enhancing electromagnetic interference shielding performance and thermal conductivity of polyvinylidene fluoride-based lamellar film with MXene and graphene," Composites, Part A **157**, 106945 (2022).
[47]Y. Cao, Z. Cheng, R. Wang, X. Liu, T. Zhang, F. Fan, and Y. Huang, "Multifunctional graphene/carbon fiber aerogels toward compatible electromagnetic wave absorption and shielding in gigahertz and terahertz bands with optimized radar cross section," Carbon **199**, 333–346 (2022).